

## Original Research Communication

# Aberrant Utilization of Nitric Oxide and Regulation of Soluble Guanylate Cyclase in Rat Diabetic Retinopathy

SILKE SCHAEFER,<sup>1,5</sup> MAYUMI KAJIMURA,<sup>1</sup> SHINGO TSUYAMA,<sup>2</sup> KOJI UCHIDA,<sup>3</sup>  
EISUKE SATO,<sup>4</sup> MASAYASU INOUE,<sup>4</sup> MAKOTO SUEMATSU,<sup>1</sup> and KENJI WATANABE<sup>5</sup>

### ABSTRACT

Although nitric oxide (NO) was shown not only to exert biological activities through activation of soluble guanylate cyclase (sGC), but also to cause oxidative stress, mechanisms for switching these pathways are unknown. This study aimed to examine aberrant utilization of NO under disease conditions such as diabetes mellitus. Diabetes was induced in male Wistar rats by injecting streptozotocin (STZ; 50 mg/kg body weight, i.p.). Retina was perfusion-fixed for immunohistochemistry to detect the gas-mediated activation of sGC by anti-sGC antibodies that are function-sensitive [monoclonal antibody (MoAb) 3221] and -insensitive (MoAb28131). Regional lipid peroxidation was also examined by an anti-acrolein MoAb. At 6 weeks after STZ injection, inducible NO synthase induction became evident, coinciding with the overproduction of nitrotyrosine, followed by that of acrolein. Despite such NO overproduction, sGC did not exhibit any notable activation. When STZ-treated animals were posttreated with a derivative of superoxide dismutase that stays in circulation without undergoing renal ultrafiltration, immunoreactivities to MoAb3221 but not to MoAb28131 increased markedly in diabetic retina, suggesting that superoxide cancels free NO for local sGC activation. These results provide evidence of aberrant utilization of NO and suggest that superoxide plays a role in interfering with NO-mediated sGC activation for phototransducing events in this neural tissue. *Antioxid. Redox Signal.* 5, 457–465.

### INTRODUCTION

**P**ROLONGED HYPERGLYCEMIA is the key feature of diabetes mellitus and stands, if left untreated, at the origin of the development of diabetic complications. Retinopathy is such a serious complication of diabetes. There is evidence that this pathologic event is triggered by varied reactive oxygen species. Under diabetic conditions, the elevated blood sugar levels lead to nonenzymatic glycation of proteins. Glycation of target proteins such as superoxide dismutase (SOD) is thought to result in impairment of elimination of superoxide

anion ( $O_2^-$ ) (29). Superoxide anion is readily cancelled by nitric oxide (NO). However, when amounts of these radicals are high, the reaction forms considerable amounts of peroxy-nitrite ( $ONOO^-$ ) that could cause tissue injury (19). Thus, the ability of tissues to generate NO could determine susceptibility of the peroxynitrite-dependent injury mechanisms.

Because of the nature to use cyclic GMP (cGMP) to exert phototransduction, retina has abundant sources of guanylate cyclase (GC). Cell types responsible for GC expression have recently been established. Retinal GC is a particulate isozyme of GC that occurs mainly in photoreceptors (6), whereas the

<sup>1</sup>Department of Biochemistry and Integrative Medical Biology, Keio University School of Medicine, Tokyo, Japan.

<sup>2</sup>Department of Veterinary Science, Osaka Prefecture University, Osaka, Japan.

<sup>3</sup>Laboratory of Food and Biodynamics, Nagoya University Graduate School of Bioagricultural Sciences, Nagoya, Japan.

<sup>4</sup>Department of Biochemistry and Molecular Pathology, Osaka City University, Medical School, Osaka, Japan.

<sup>5</sup>Department of Oriental Medicine, Keio University School of Medicine, Tokyo, Japan.

GC in the second neuron such as bipolar cells and in Müller's glia cells (MGCs) is the soluble form (13). This soluble isozyme is a receptor for NO, which is activated by binding the gas to the prosthetic heme (13). Once bound to the heme, NO triggers conformational changes essential for increasing the cyclase activities to generate cGMP. Under physiologic conditions, the sites of NO generation in this organ have also been revealed; microvascular endothelial cells spreading over the inner layers of retina, as well as a subpopulation of amacrine cells, express endothelial NO synthase (NOS) and neuronal NOS, respectively, whereas the outer cell layers such as the external limiting membrane (ELM) and outer segments of the photoreceptor layer express little NOS, if any (13). Thus, NO-mediated oxidative stress in diabetic retinopathy could take place in a site-specific manner, and determination of such primary lesion deserves extensive studies to understand the pathophysiology of this diabetic complication. The aim of this study is to visually assess alterations in NO generation and their functional outcomes on soluble GC (sGC) activation and nitrosyl stress in diabetic retinopathy. To visualize functional alterations in sGC, we applied a novel monoclonal antibody (MoAb) that recognizes a regiospecific epitope critical for NO-mediated activation of the enzyme through immunohistochemistry (13, 26).

## MATERIALS AND METHODS

### *Animal experiments*

All animal experiments were performed with the approval of and in accordance with the recommendations of the Animal Care and Utilization Committee of Keio University School of Medicine. Male adult Wistar rats (260–280 g) were kept under a half-day light and dark cycle at an ambient temperature of 22–23°C. Free access to water and standard chow was provided except for an overnight fast before triggering diabetes by a single intraperitoneal injection of streptozotocin (STZ, 50 mg/kg body weight; Sigma, Tokyo, Japan) dissolved in 0.1 M citrate buffer (pH 4.5). A control group was given an intraperitoneal injection of the citrate buffer (pH 4.5) after a similar fast. Blood sugar levels were measured at regular intervals, and drinking water consumption was monitored daily. Diabetic blood sugar levels were determined on the following days. Rats with blood sugar levels of <300 mg/dl were not included in the study.

After 6 and 12 weeks, rats were anesthetized by intraperitoneal injection of pentobarbital sodium (Somnopenyl; KS, Tokyo, Japan). The chest cavity was opened, and a 21-gauge needle was inserted into the left ventricle. A cut was made into the right atrium to allow outflow of blood and perfusate. Rats were then perfused with phosphate-buffered saline (PBS) for 4 min (40 ml/min), followed by 3-min perfusion with 4% paraformaldehyde in PBS. The eyes were then prepared and the parietotemporal pole was marked with ophthalmic silk (0.4 metric; Mani Sutures, Japan) for orientation. Eyes were enucleated, and retinal cups were prepared carefully under the microscope and immersion-fixed for 1 h in 4% paraformaldehyde on ice. Cryoprotection was done through increasing concentrations of sucrose solutions (6%, 12%, 24%, and 30% overnight).

The prepared eyecups were then embedded in O.C.T compound (Tissue-tek, Sakura, Japan), frozen with liquid nitrogen, and stored at –80°C.

### *Immunohistochemistry*

For immunostaining, 7- $\mu$ m-thick slices were cut along the temporal–nasal axis, including the optic nerve head in the middle. Immunohistochemistry was carried out using an avidin-biotinylated enzyme complex system (Vectastain Elite ABC kit; Vector Laboratories, Burlingame, CA, U.S.A.). Sections were rehydrated and washed twice for 10 min each time with PBS–Triton (0.1%) and PBS. The sections were subsequently incubated for 30 min with a serum of the secondary antibody, to block nonspecific binding sites of the biotinylated antibody. Afterwards, sections were drained and incubated for 2 h with the primary antibody, diluted in 1% bovine serum albumin/PBS–Triton. After washing of the sections once more in PBS–Triton and thereafter for three times with PBS (5 min for each wash), endogenous peroxidase activity was blocked by 15-min incubation in 0.3% hydrogen peroxide in methanol. After another washing step, the sections were incubated with the avidin-biotin/horseradish peroxidase complex for 30 min. Sections were then washed and developed in a diaminobenzidine (Dojindo, Kumamoto, Japan) solution containing hydrogen peroxide for 11 min. The sections were again washed thoroughly and fixed with 20% formaldehyde for 10 min. They were counterstained with methyl green for 10 min, and washed again. Then sections were dehydrated through ethanol, cleared with xylene, and mounted in a hydrophobic mounting medium. Negative control staining was performed by omission of the primary antibody, and nonspecific staining was tested by incubation of the sections with the immunoglobulin of the primary antibody.

Regional lipid peroxidation was tested with an anti-acrolein MoAb5F6 (2  $\mu$ g/ml), which recognizes an epitope of the product yielded by the reaction of acrolein with amino groups of the protein (27, 28). For nitrosyl stress, we stained with the anti-nitrotyrosine (anti-NO<sub>2</sub>-Y) antibody (4  $\mu$ g/ml; Upstate Biotechnology, Lake Placid, NY, U.S.A.). This antibody recognizes nitrated tyrosine residues that are generated from peroxynitrite (20, 21). Generation sites of NO were examined by antibodies against inducible NOS (iNOS; 5  $\mu$ g/ml, Chemicon International, Temecula, CA, U.S.A.) and endothelial NOS (2  $\mu$ g/ml, Transduction Laboratories, Lexington, KY, U.S.A.). The gas-mediated activation of sGC was tested using MoAb3221 and MoAb28131. MoAb3221 is a function-sensing MoAb binding to a regiospecific region of sGC that is constituted by both the  $\alpha$  and  $\beta$  subunits of the enzyme; upon binding of NO to the prosthetic heme of the  $\beta$  subunit, the affinity between the antibody and sGC becomes 100-fold greater than that in the absence of NO (26). Such a feature of the MoAb3221 turned out to be applicable to immunohistochemical detection of the sGC activation *in vivo* as described in our recent study (13, 26). Staining with this antibody at 30  $\mu$ g/ml was compared with MoAb28131 (50  $\mu$ g/ml), an antibody that binds to the  $\beta$  subunit of sGC alone and whose binding is therefore independent of enzyme-activation.

When necessary, the human erythrocyte-type SOD derivative, styrene-co-maleic acid (SM)-SOD (5 mg/kg body

weight) was administered at the desired doses for 3 days, twice daily before killing at 6 weeks of diabetes. SM-SOD was prepared as described previously (12). In brief, the compound was synthesized by covalently linking poly(styrene-co-maleic acid) butyl ester to a copper/zinc-type SOD. The circulation half-life of this compound is  $\sim 6$  h, in contrast to a feature of naturally occurring SOD whose half-life is only 5 min, if injected intravenously (12). Under these conditions, no reduction of blood sugar level was evident, *i.e.*, the blood sugar levels of these animals were  $>600$  mg/ml, comparable to those of untreated animals.

As shown later, diabetic insult turned out to cause an increase in the stripe-like processes with heavy  $\text{NO}_2\text{-Y}$  immunoreactivities in the inner plexiform layer (IPL). The densities of such stripe-like structures were determined morphometrically.

### Evaluation of site-specific changes of immunoreactivities in retina

Site-specific changes in immunoreactivities among retinal cell layers were evaluated according to previously established protocols with modifications (17). In brief, histological micrographs were put into the color image processors, where the color images were divided into red, green, and blue components, with each component graded for brightness from 1 (darkest) to 256 (brightest). To use the intensities of the chromogen formed by the diaminobenzidine–horseradish peroxidase reaction as an index of immunoreactivities, nuclear counterstaining with methyl green had to be eliminated. To do so, the levels for red, green, and blue components to define color of methyl green were subtracted. After these subtractions, images were converted into gray levels. For each image, gray levels were measured in five different domains of the retina; these domains were the ganglion cell layer (GCL), IPL, inner nuclear layer (INL), outer nuclear layer (ONL), and the area just above the ELM. Under the defined conditions where we examined immunoreactivities for each of the antibodies, no converted images of 8-bit gray level reached saturation. To avoid bias in image analysis, an algorithm was developed to detect automatically the structure of the layers and place five boxes automatically along each evaluated layer of the retina.

### Statistics

Values are expressed as means  $\pm$  SE unless stated otherwise. Significant differences between means were evaluated using ANOVA followed by Fisher's test. Differences of  $p < 0.05$  were considered statistically significant.

## RESULTS

### Formation of lipid peroxidation, peroxynitrite, and iNOS expression in diabetic retina

To assess tissue damage in the diabetic retina, we first examined lipid peroxidation. Figure 1 illustrates the distribution of immunoreactivities to anti-acrolein MoAb5F6, a marker for lipid peroxidation (27, 28). As seen in Fig. 1A, the control

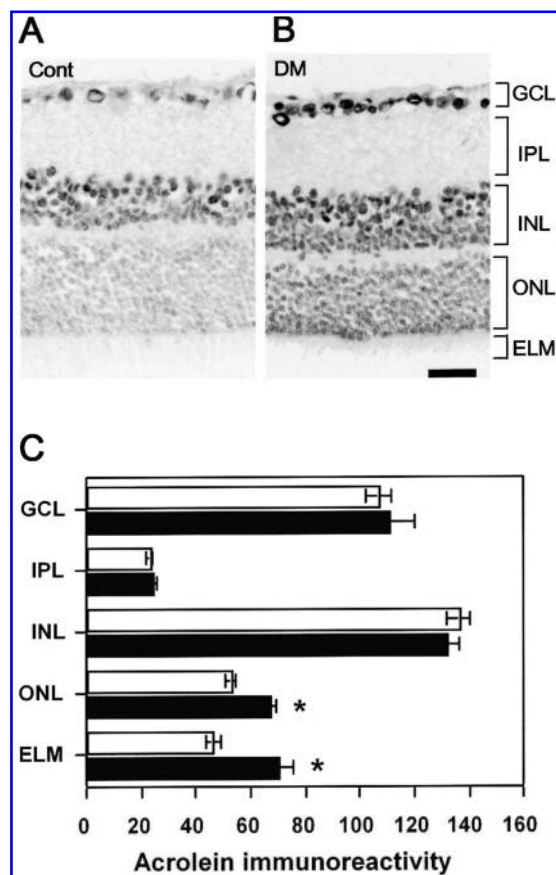


**FIG. 1. Increased lipid peroxidation in diabetic retina immunohistochemically detected with anti-acrolein antibody.** (A) Vehicle-treated control. (B) At 12 weeks after the initial injection of STZ. DM, diabetes mellitus. (C) Layer-specific changes of acrolein immunoreactivity expressed as gray level in control (open columns) and DM (filled columns) groups. Scale bar = 25  $\mu\text{m}$ . \* $p < 0.05$ , an increase as compared with vehicle-treated control. Values are means  $\pm$  SE.

retina expressed rather weak MoAb5F6-associated immunoreactivity. By contrast, at 12 weeks after induction of diabetes, immunoreactivities were markedly increased in ONL and ELM. This enhancement was confirmed by immunohistochemical densitometry shown in Fig. 1C. ELM and ONL where distal processes of MGCs reside exhibited 25% and 50% increases in MoAb5F6-associated immunoreactivities, respectively, and these changes were found to be greater than those in other layers of retina examined.

This observation led us to examine if increased levels of peroxynitrite caused the elevated formation of lipid peroxidation. To this end, we used anti- $\text{NO}_2\text{-Y}$  antibody as a marker of posttranslational modification of proteins by NO-derived oxidant peroxynitrite (3, 20, 21). In control retina, only weak immunoreactivities were seen in the entire depth of retinal layers. At 12 weeks after the STZ administration, however, the staining pattern changed dramatically. As seen in arrowheads in Fig. 2B, the most notable positive immunoreactivities appeared as stripe-like structure in IPL, and the enhancement

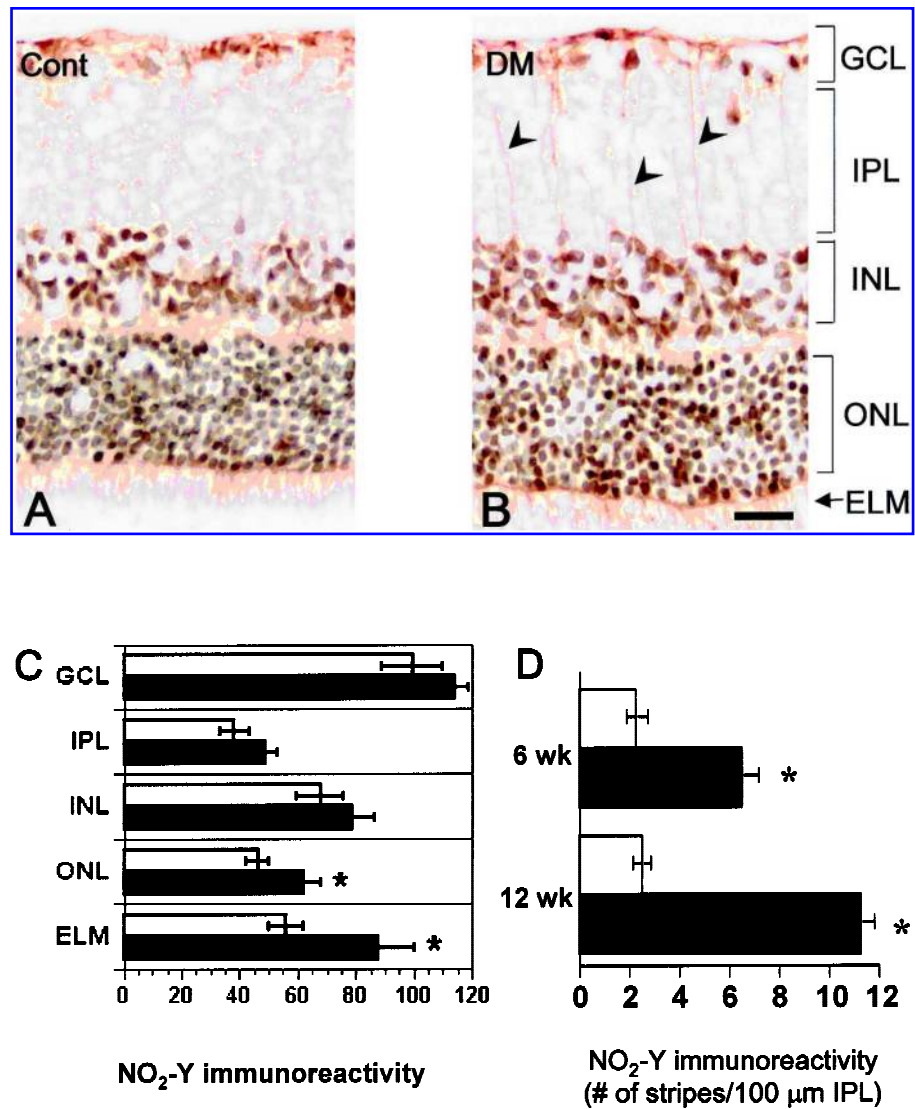


**FIG. 2. Increased peroxynitrite formation in diabetic retina immunohistochemically detected with anti-NO<sub>2</sub>-Y antibody.** (A) Vehicle-treated control. (B) At 12 weeks after the initial injection of STZ. Note the stripe-like structure in IPL (arrowheads). DM, diabetes mellitus. (C) Layer-specific changes of NO<sub>2</sub>-Y immunoreactivity expressed as gray level in control (open columns) and DM (filled columns) groups. (D) NO<sub>2</sub>-Y immunoreactivity expressed as the number of stripe-like structures in IPL. Scale bar = 25 μm. \**p* < 0.05, an increase as compared with vehicle-treated control. Values are means ± SE.

was evident in ONL and ELM. This staining pattern distributing over the different layers of retina from GCL to ELM suggests that the MGC is the site for lipid peroxidation. Layer-specific changes in NO<sub>2</sub>-Y immunoreactivities shown in Fig. 2C were similar to those observed with MoAb5F6 staining in that the relative increase at ELM (55%) was the greatest among all domains examined. When the density of stripe-like structure in IPL was counted, significant increase was found in the diabetic retina at both 6 and 12 weeks as compared with that in the normal retina (Fig. 2D).

We then examined whether increased formation of peroxynitrite attributed to an increase in iNOS expression and subsequent overproduction of NO in the diabetic retina. The expression of iNOS was increased compared with that in the control retina (Fig. 3), consistent with a previous study (1).

Figure 3D shows that iNOS occurred in the cells extending processes (arrowheads) over GCL down to IPL, a very similar pattern to the NO<sub>2</sub>-Y immunoreactivities (Fig. 2B), suggesting its expression in MGCs. These observations indicate that the site for sensing oxidative stress could be at these glial cells.

*Absence of sGC activation in diabetic retina*

We examined if up-regulation of NO production enhances local activities of a receptor protein, sGC. This enzyme is expressed in MGCs and on-type bipolar cells in the rat retina under normal conditions (13). To visualize local alterations in activation states of sGC under diabetic conditions, we used two MoAbs against the enzymes, MoAb28131 and

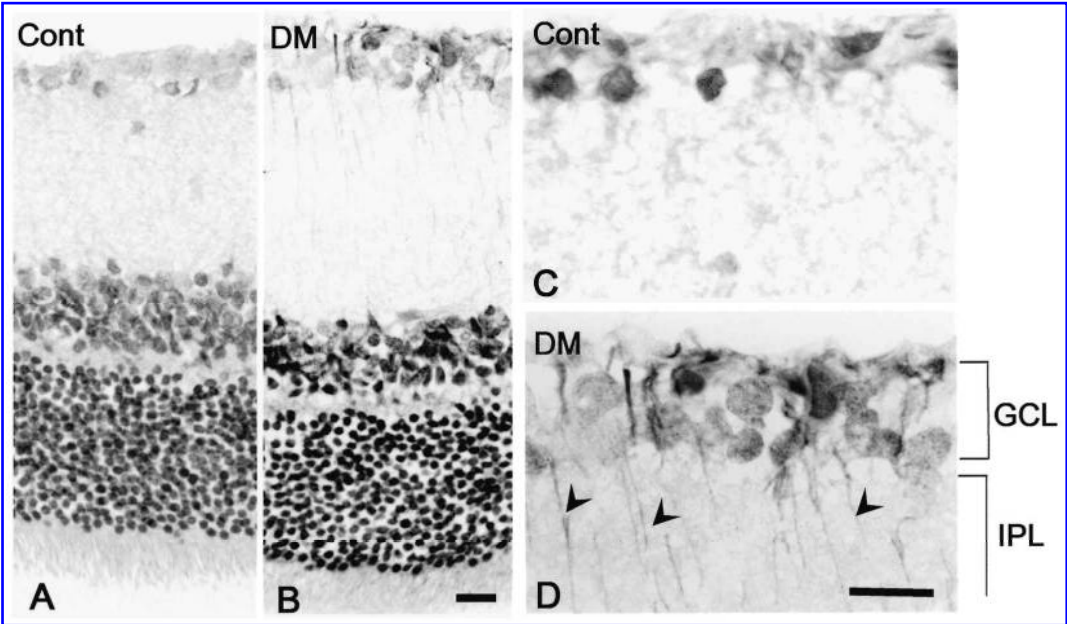


**FIG. 3. Immunohistochemical staining for iNOS of the rat retina.** (A) Vehicle-treated control. (B) At 6 weeks after the initial injection of STZ. DM, diabetes mellitus. (C and D) High-magnification images of control and STZ-treated groups, respectively. Note the stripe-like structures in IPL (arrowheads). Scale bar = 20  $\mu$ m.

MoAb3221. Previous studies in our laboratory (13) showed that, in the presence of NO, MoAb3221 increases its affinity to sGC by ~100-fold *in vitro*, indicating its ability to sense gas reception. By contrast, MoAb28131 shows no change in the affinity to sGC. As seen in Fig. 4, there was no difference in MoAb3221-associated immunoreactivities between the control and the 6-week diabetic retina, suggesting that overproduction of NO did not cause a notable increase in sGC activities. MoAb3221-associated immunoreactivities, but not MoAb28131-associated ones, were enhanced in the control retina after the intravenous administration of L-arginine (70  $\mu$ mol/kg body weight), confirming results of the previous study (13) that MoAb3221 can detect changes in the sGC activities in retinal tissues (data not shown).

*Restoration of sGC activation by SOD administration*

Aforementioned observation led us to hypothesize that near diffusion-limited interaction with superoxide anions and NO forming peroxynitrite dissipates overproduced NO before it binds to the heme moiety of sGC. We thus attempted to increase NO bioavailability by eliminating local superoxide anions and to examine MoAb3221 immunoreactivities as an index of the sGC activities *in situ*. To this end, SM-SOD (5 mg/kg body weight) (12) was administered intravenously to the diabetic rats twice daily for 3 days prior to killing. Such treatment to reduce superoxide anions resulted in enhancement of MoAb3221 immunoreactivities over several different regions of retina, including GCL, INL, ONL, and ELM (Fig. 5A and B). On the other hand, adding SOD in circulation for this short duration did not cause any changes in iNOS and NO<sub>2</sub>-Y immunoreactivities (data not shown). Considering that the MoAb28131 immunoreactivities were not altered

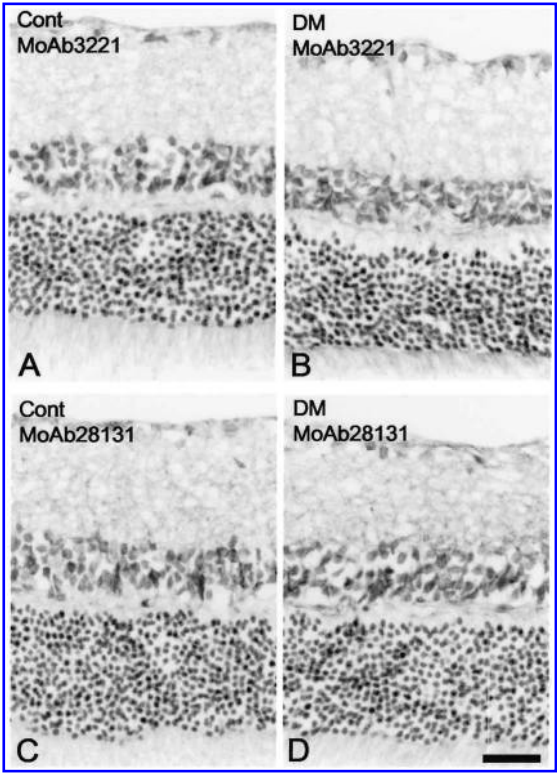


**FIG. 4. Visualization of sGC activities at 6 weeks after the induction of diabetes.** (A and B) Immunoreactivities to MoAb3221, which detects both  $\alpha$  and  $\beta$  subunits of sGC and acquires a greater binding affinity upon enzyme activation. DM, diabetes mellitus. (C and D) Immunoreactivities to MoAb28131, which recognizes the  $\beta$  subunit of the enzyme. Note no evident difference in staining pattern between the vehicle-treated control and DM groups. Scale bar = 25  $\mu$ m.

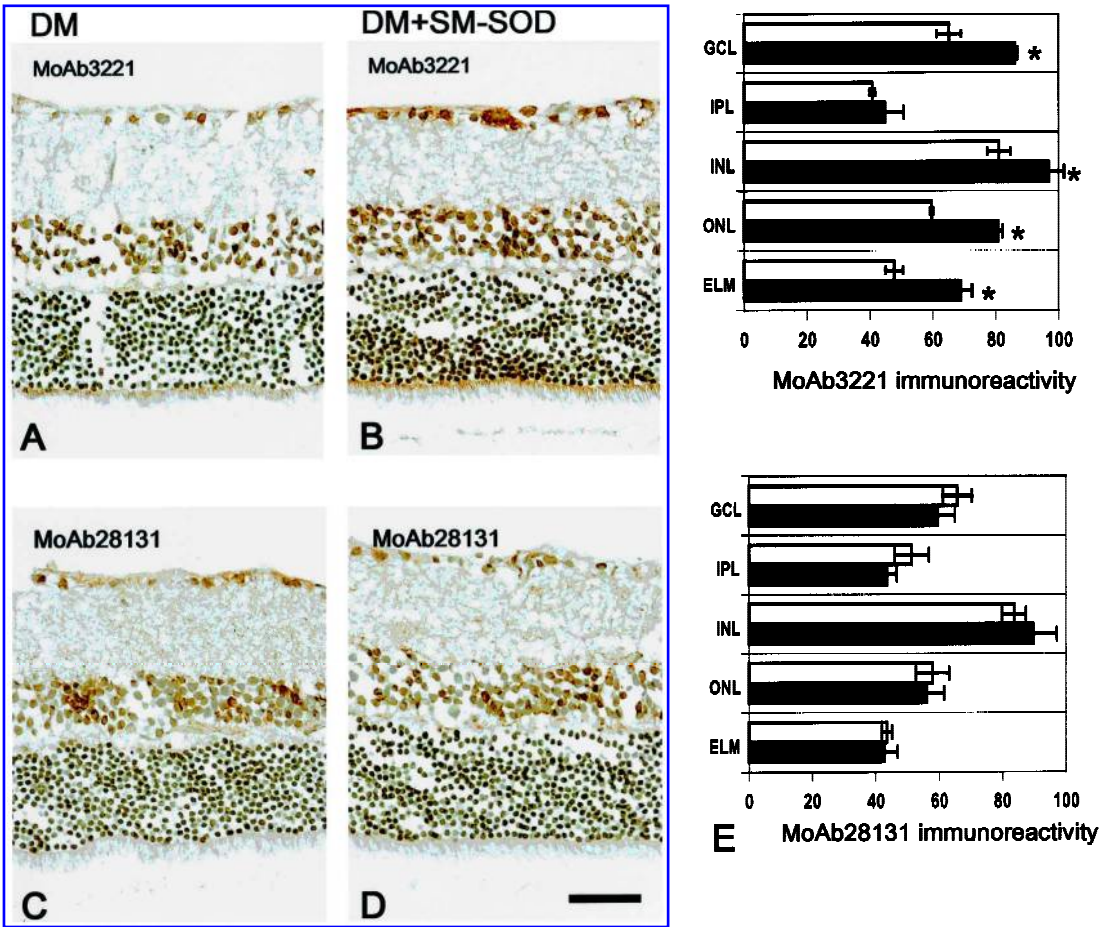


**FIG. 5. Enhanced sGC activities in the diabetic retina after SM-SOD treatment.** (A and C) The 6-week diabetes mellitus (DM) retina that received PBS only. (B and D) The DM retina after the intravenous administration of SM-SOD. Note the increase in MoAb3221-associated immunoreactivity in the SM-SOD group. (E) Layer-specific changes of sGC immunoreactivities in PBS- (open columns) and SOD-treated (filled columns) groups. Scale bar = 25  $\mu$ m. \* $p$  < 0.05, an increase as compared with the PBS-treated group. Values are means  $\pm$  SE.

with the same protocol for administration of SM-SOD (Fig. 5C and D), these data suggest that locally generated superoxide anions caused the absence of sGC activation under NO-overproducing conditions in the diabetic retina. Patterns of layer-specific increases in MoAb3221-associated immunoreactivities in the SM-SOD group (Fig. 5E, top panel) were similar to those observed with MoAb5F6-associated and NO<sub>2</sub>-Y immunoreactivities in that relative enhancements in ELM and ONL (45% and 35%, respectively) were greater than those in other layers such as IPL and INL (10% and 20%, respectively).

DISCUSSION

The current study provided evidence of the up-regulation of iNOS in a glial component of the retinal tissue undergoing diabetes mellitus. Furthermore, free NO available for sGC in the cell turned out to be limited because of cancellation of the gas by local superoxide generation. As a result of these

events, inducible NO results in nitrosylation of tyrosine residues of proteins at as early as 6 weeks after the administration of STZ. At a later period such as 12 weeks, ONL and ELM were finally exposed to notable enhancement of lipid peroxidation. During these periods of time, the fundamental structure of the retinal cell layers remained apparently intact, suggesting that the NO-mediated NO<sub>2</sub>-Y generation and lipid peroxidation are primary events of diabetic retinopathy that occur prior to the onset of anatomical remodeling of the tissue.

Careful consideration of the current data shed light on two distinct topographic features of early events of oxidative injury during diabetic retinopathy: cell types and layer specificity. Considering the anatomical features of NO<sub>2</sub>-Y-positive cells and localization of sGC, MGCs obviously constitute a major cell type responsible for nitroxidative stress in this experimental model. This notion is well supported by previous observation showing an increase in NO<sub>2</sub>-Y formation in either retinal homogenates of diabetic rats or cultured MGCs incubated at high glucose concentrations (7). Furthermore,

oxidative changes occurring in MGCs were obviously heterogeneous among different levels of the retinal cell layers. Several features of layer-specific events were detectable from the current semiquantitative densitometric analyses. First, the IPL showed absolutely no changes in lipid peroxidation judged by the acrolein immunoreactivities. Second, the same layer did not exhibit any notable restoration of the NO-mediated activation of sGC by cancellation of local superoxide generation. Finally and most importantly, ELM exhibited the most prominent changes in immunoreactivities of all oxidative parameters such as acrolein and NO<sub>2</sub>-Y, and the same domain displayed the largest restoration of sGC activation among different cell layers, upon cancellation of superoxide anions. These results first provided evidence that the ELM domain of MGCs serves as a portion most susceptible to diabetic impacts.

Mechanisms for such microtopographic specificity of the NO-mediated oxidative events have not been fully revealed in the current study. It is, however, not unreasonable to hypothesize that polarity of oxygen consumption in portions of the cell body in MGCs and/or heterogeneity in local oxygen tension could determine spatially distinct features of NO-mediated oxidative changes. As previously documented in MGCs isolated from the salamander, mitochondrial density judged by NAD(P)H autofluorescence is much more intense in the distal processes, consisting of ONL and ELM, than in either the soma or the endofoot of MGCs (18, 25); thus, redox states are different between the perinuclear cell body and distal processes of the same MGC. Namely, INL, which includes the cell body of MGCs, seems to exhibit greater consumption of molecular oxygen than IPL, where none of the cell bodies were localized. On the other hand, ONL and ELM contain photoreceptors that could constitute another major cell compartment for the oxygen consumption. As the microvascular density in these layers is the smallest among retinal layers, this domain could be most susceptible to a shortage of oxygen and nutritional supply. Furthermore, because of the nature of NO, the half life of which greatly depends on local oxygen tension, the gas generated by iNOS in relatively inner layers of the retina could diffuse easily into the outer layers and aggravate nitrooxidative stress in ONL and/or ELM. Further investigation is obviously necessary to unravel the whole picture of the gas-mediated oxidative changes in this model. However, the current study suggested that ONL and ELM domains of MGCs serve as a primary target of oxidative stress of diabetic retinopathy and shed light on the possibility that the primary pathogenic event could occur in the deeper portion of retina distal from the inner surface of the retina where clinicians can observe the changes through an ophthalmoscope.

Clinically relevant lesions caused by diabetes in the retina have been shown to occur in blood vessels involving microvascular pericytes (11, 30). However, evidence that retinal neuroglial abnormalities occur before the characteristic lesions of diabetic microangiopathy continues to mount up (16), and our results support this. One of the most prominent neuronal abnormalities of this kind is the changes in the pattern and level of expression of glial fibrillary acidic protein in activated MGCs. To date, the relationship between early onset of neuroglial and vascular abnormalities is obscure. Recent

literature, however, suggests that vascular endothelial growth factor is produced by MGCs of human with nonproliferative diabetic retinopathy (2) and of the rat (9). Considering that MGCs are located between retinal neurons and microvascular endothelium and constitute the blood-retinal barrier, further investigation is necessary to unravel the pathophysiologic link between glial activation and microvascular damage (e.g., pericyte apoptosis).

Maintenance of functional integrity of sGC activation in MGCs has been considered as a clue to keep homeostasis of phototransduction and neuroglial interactions in neural tissues. MGCs express cGMP-gated channels (14), and through these channels cGMP is involved in regulating uptake and recycling of glutamate released from neurons into the interstitium. On the other hand, excess amounts of cGMP in cells have recently been shown to trigger apoptosis (5, 8). Furthermore, factors that regulate sGC activities were not only local concentrations of free NO available for the prosthetic heme of the enzyme, but carbon monoxide generated from heme oxygenase, a neurovascular signaling molecule (10, 15, 22–24). It was actually demonstrated *in vitro* that sGC can be activated by carbon monoxide and inhibited directly by superoxide anions through mechanisms independent of NO (4). Our finding that SM-SOD administration restores sGC activities suggests that keeping adequate SOD activities in circulation plays an important role in maintaining cGMP homeostasis in MGCs, and possible glycation of this enzyme could cause a dysfunction of glial activities. Future investigation should be awaited to reveal roles of the whole regulatory elements played in homeostasis of phototransduction, and sources of superoxide generation operated during the developmental processes of diabetic retinopathy.

## ACKNOWLEDGMENTS

We thank Robert Cameron, Science University of Tokyo, for his contribution in relation to the Computer Analysis Program and Kazunari Kondo for his technical assistance. S.S. was supported by a joint grant of the German Alexander-von-Humboldt Foundation and the Japan Society for the Promotion of Science. This work is supported by Keio Health Counseling Center Funds, Grant-in-Aid for Creative Scientific Research (13GS0015) in Health Science Research grants for Research on Advanced Medical Technology from the Ministry of Health and Welfare in Japan, and The Leading Project for Biosimulation grant for the 21<sup>st</sup> Century Center-of-Excellence Program from the Ministry of Education and Sciences Technology in Japan.

## ABBREVIATIONS

cGMP, cyclic GMP; ELM, external limiting membrane; GC, guanylate cyclase; GCL, ganglion cell layer; INL, inner nuclear layer; IPL, inner plexiform layer; iNOS, inducible nitric oxide synthase; MGCs, Müller's glial cells; MoAb, monoclonal antibody; NO, nitric oxide; NOS, nitric oxide synthase; NO<sub>2</sub>-Y, nitrotyrosine; ONL, outer nuclear layer; PBS,

phosphate-buffered saline; sGC, soluble guanylate cyclase; SM, styrene-co-maleic acid; SOD, superoxide dismutase; STZ, streptozotocin.

## REFERENCES

1. Abu El-Asrar AM, Desmet S, Meersschaert A, Dralands L, Missotten L, and Geboes K. Expression of the inducible isoform of nitric oxide synthase in the retinas of human subjects with diabetes mellitus. *Am J Ophthalmol* 132: 551–556, 2001.
2. Amin RH, Frank RN, Kennedy A, Elliott D, Puklin JE, and Abrams GW. Vascular endothelial growth factor is present in glial cells of the retina and optic nerve of human subjects with nonproliferative diabetic retinopathy. *Invest Ophthalmol Vis Sci* 38: 36–47, 1997.
3. Brennan ML, Wu W, Fu X, Shen Z, Song W, Frost H, Vadseth C, Narine L, Lenkiewicz E, Borchers MT, Lusis AJ, Lee JJ, Lee NA, Abu-Soud HM, Ischiropoulos H, and Hazen SL. A tale of two controversies: defining both the role of peroxidases in nitrotyrosine formation in vivo using eosinophil peroxidase and myeloperoxidase-deficient mice, and the nature of peroxidase-generated reactive nitrogen species. *J Biol Chem* 277: 17415–17427, 2002.
4. Brune B, Schmidt KU, and Ullrich V. Activation of soluble guanylate cyclase by carbon monoxide and inhibition by superoxide anion. *Eur J Biochem* 192: 683–688, 1990.
5. Brunetti M, Mascetra N, Manarini S, Martelli N, Cerletti C, Musiani P, Aiello FB, and Evangelista V. Inhibition of cGMP-dependent protein kinases potently decreases neutrophil spontaneous apoptosis. *Biochem Biophys Res Commun* 297: 498–501, 2002.
6. Dizhoor AM. Regulation of cGMP synthesis in photoreceptors: role in signal transduction and congenital diseases of the retina. *Cell Signal* 12: 711–719, 2000.
7. Du Y, Smith MA, Miller CM, and Kern TS. Diabetes-induced nitrate stress in the retina, and correction by aminoguanidine. *J Neurochem* 80: 771–779, 2002.
8. Ferrero R and Torres M. Prolonged exposure to YC-1 induces apoptosis in adrenomedullary endothelial and chromaffin cells through a cGMP-independent mechanism. *Neuropharmacology* 41: 895–906, 2001.
9. Gerhardinger C, Brown LF, Roy S, Mizutani M, Zucker CL, and Lorenzi M. Expression of vascular endothelial growth factor in the human retina and in nonproliferative diabetic retinopathy. *Am J Pathol* 152: 1453–62, 1998.
10. Goda N, Suzuki K, Naito M, Takeoka S, Tsuchida E, Ishimura Y, Tamatani T, and Suematsu M. Distribution of heme oxygenase isoforms in rat liver. Topographic basis for carbon monoxide-mediated microvascular relaxation. *J Clin Invest* 101: 604–612, 1998.
11. Hammes HP, Lin J, Renner O, Shani M, Lundqvist A, Betsholtz C, Brownlee M, and Deutsch U. Pericytes and the pathogenesis of diabetic retinopathy. *Diabetes* 51: 3107–3112, 2002.
12. Inoue M, Ebashi I, Watanabe N, and Morino Y. Synthesis of a superoxide dismutase derivative that circulates bound to albumin and accumulates in tissues whose pH is decreased. *Biochemistry* 28: 6619–6624, 1989.
13. Kajimura M, Shimoyama M, Tsuyama S, Suzuki T, Kozaki S, Takenaka S, Tsubota K, Oguchi Y, and Suematsu M. Visualization of gaseous monoxide reception by soluble guanylate cyclase in the rat retina. *FASEB J* 17: 506–508, 2003.
14. Kusaka S, Dabin I, Barnstable CJ, and Puro DG. cGMP-mediated effects on the physiology of bovine and human retinal Müller (glial) cells. *J Physiol* 497: 813–824, 1996.
15. Kyokane T, Norimizu S, Taniai H, Yamaguchi T, Takeoka S, Tsuchida E, Naito M, Nimura Y, Ishimura Y, and Suematsu M. Carbon monoxide from heme catabolism protects against hepatobiliary dysfunction in endotoxin-treated rat liver. *Gastroenterology* 120: 1227–1240, 2001.
16. Lorenzi M and Gerhardinger C. Early cellular and molecular changes induced by diabetes in the retina. *Diabetologia* 44: 791–804, 2001.
17. Morikawa N, Suematsu M, Kyokane T, Goda N, Kumamoto Y, Okitsu T, Ishimura Y, and Kitajima M. Discontinuous total parenteral nutrition prevents postischemic mitochondrial dysfunction in rat liver. *Hepatology* 28: 1289–1299, 1998.
18. Poitry S, Poitry-Yamate C, Ueberfeld J, MacLeish PR, and Tsacopoulos M. Mechanisms of glutamate metabolic signaling in retinal glial (Müller) cells. *J Neurosci* 20: 1809–1821, 2000.
19. Pryor WA and Squadrito GL. The chemistry of peroxynitrite: a product from the reaction of nitric oxide with superoxide. *Am J Physiol* 268: L699–L722, 1995.
20. Sawa T, Akaike T, and Maeda H. Tyrosine nitration by peroxynitrite formed from nitric oxide and superoxide generated by xanthine oxidase. *J Biol Chem* 275: 32467–32474, 2000.
21. Shibuki H, Katai N, Yodoi J, Uchida K, and Yoshimura N. Lipid peroxidation and peroxynitrite in retinal ischemia-reperfusion injury. *Invest Ophthalmol Vis Sci* 41: 3607–3614, 2000.
22. Suematsu M and Ishimura Y. The heme oxygenase–carbon monoxide system: a regulator of hepatobiliary function. *Hepatology* 31: 3–6, 2000.
23. Suematsu M, Tamatani T, Delano FA, Miyasaka M, Forrest M, Suzuki H, and Schmid-Schonbein GW. Microvascular oxidative stress preceding leukocyte activation elicited by in vivo nitric oxide suppression. *Am J Physiol* 266: H2410–H2415, 1994.
24. Suematsu M, Goda N, Sano T, Kashiwagi T, Egawa T, Shinoda Y, and Ishimura Y. Carbon monoxide: an endogenous modulator of sinusoidal tone in the perfused rat liver. *J Clin Invest* 96: 2431–2437, 1995.
25. Tsacopoulos M, Poitry-Yamate CL, MacLeish PR, and Poitry S. Trafficking of molecules and metabolic signals in the retina. *Prog Retin Eye Res* 17: 429–442, 1998.
26. Tsuyama S, Yamazaki E, Tomita T, Ihara T, Takenaka S, Kato K, and Kozaki S. Characterization of a novel monoclonal antibody that senses nitric oxide-dependent activation of soluble guanylate cyclase. *FEBS Lett* 455: 291–294, 1999.

27. Uchida K, Kanematsu M, Morimitsu Y, Osawa T, Noguchi N, and Niki E. Acrolein is a product of lipid peroxidation reaction. Formation of free acrolein and its conjugate with lysine residues in oxidized low density lipoproteins. *J Biol Chem* 273: 16058–16066, 1998.
28. Uchida K, Kanematsu M, Sakai K, Matsuda T, Hattori N, Mizuno Y, Suzuki D, Miyata T, Noguchi N, Niki E, and Osawa T. Protein-bound acrolein: potential markers for oxidative stress. *Proc Natl Acad Sci U S A* 95: 4882–4887, 1998.
29. Wolin MS and Mohazzab-H KM. Mediation of signal transduction by oxidants. In: *Oxidative Stress and the Molecular Biology of Antioxidant Defenses*, edited by Scandalios JG. Plainview, NY: Cold Spring Harbor Laboratory Press, 1997, pp. 21–48.
30. Yamagishi S, Inagaki Y, Amano S, Okamoto T, Takeuchi M, and Makita Z. Pigment epithelium-derived factor protects cultured retinal pericytes from advanced glycation end product-induced injury through its antioxidative properties. *Biochem Biophys Res Commun* 296: 877–882, 2002.

Address reprint requests to:

Dr. Silke Schaefer, M.A.

Department of Gastroenterology and Endocrinology

Universitätsklinik Goettingen

Robert-Koch-Strasse 40

37075 Goettingen

Germany

E-mail: silke@med.uni-goettingen.de

Received for publication February 23, 2003; accepted March 19, 2003.

**This article has been cited by:**

1. Betty K. Samulitis, Terry H. Landowski, Robert T. Dorr. 2006. Correlates of imexon sensitivity in human multiple myeloma cell lines. *Leukemia & Lymphoma* **47**:1, 97-109. [[CrossRef](#)]
2. Silke Cameron-Schaefer, Kazunari Kondo, Atsushi Ishige, Shingo Tsuyama, Koji Uchida, Toshihiko Hanawa, Makoto Suematsu, Kenji Watanabe. 2006. Maintaining the Redox-Balance Intact: Gosha-Jinki-Gan but Not Insulin Activates Retinal Soluble Guanylate Cyclase in Diabetic Rats. *Ophthalmic Research* **38**:2, 95-104. [[CrossRef](#)]
3. Mariano J. Taverna, Fabienne Elgrably, Henri Selmi, Jean-Louis Selam, Gérard Slama. 2005. The T-786C and C774T endothelial nitric oxide synthase gene polymorphisms independently affect the onset pattern of severe diabetic retinopathy. *Nitric Oxide* **13**:1, 88-92. [[CrossRef](#)]
4. Makoto Suematsu . 2003. Quartet Signal Transducers in Gas Biology. *Antioxidants & Redox Signaling* **5**:4, 435-437. [[Citation](#)] [[PDF](#)] [[PDF Plus](#)]